Available online at www.sciencedirect.com
SCIENCE DIRECT®
Journal of Organometallic Chemistry 690 (2005) 5736–5746
Journal of Organometallic Chemistry
www.elsevier.com/locate/jorganchem

Rhodium *N*-heterocyclic carbene complexes: Synthesis, structure, NMR studies and catalytic activity

Daryl P. Allen [a], Cathleen M. Crudden [a,*], Larry A. Calhoun [b], Ruiyao Wang [a,1], Andreas Decken [b,1]

[a] *Department of Chemistry, Queen's University, Kingston, Ont., Canada K7L 3N6*
[b] *Department of Chemistry, University of New Brunswick, Fredericton, New Brunswick, Canada E3B 6E2*

Received 10 June 2005; accepted 8 July 2005
Available online 22 August 2005

Abstract

The solid state structure, phosphine dissociation rates and catalytic activity of several Rh-*N*-heterocyclic carbene complexes were studied. Catalytic activity for the hydrogenation of β-methylstyrene was improved by up to two orders of magnitude upon the addition of copper chloride. The catalyst with the highest inherent activity was found to be [Rh(IMes)(P-*p*-$FC_6H_4)_3$], although the *p*-methoxy derivative benefited the most from the addition of CuCl, giving turnover numbers of over 400 h^{-1}.
© 2005 Published by Elsevier B.V.

Keywords: *N*-heterocyclic carbene; Catalysis; Hydrogenation; Rhodium; Phosphine exchange; Saturation transfer

1. Introduction

N-heterocyclic carbenes (NHCs) have been found to be useful alternatives to phosphines in many catalytic reactions, of which coupling reactions and olefin metathesis are likely the most significant [1,2]. Although early studies focussed mostly on the synthetic applications, mechanistic studies have demonstrated the complex effects that NHCs can have on different steps of the catalytic cycle [3,4]. One important aspect of the chemistry of NHCs is their affect on other ligands in the metal sphere. For example in the case of metathesis reactions, Grubbs and co-workers [5] showed that even though the mixed carbene/phosphine complex **2** is more active than its predecessor **1**, it actually initiates more slowly.

By measuring phosphine dissociation rates, the Grubbs group showed that phosphine dissociation in carbene complex **1** is orders of magnitude slower than it is in **2** [5]. This is somewhat counter-intuitive since the more electron rich, strongly bound carbene ligand would be expected to be a strong *trans* effect ligand, labilizing the ligand *trans* to it. However, the increased activity of the mixed complex **2** is not attributed to the rate of phosphine dissociation, but to the relative rates of olefin binding compared to recapture of phosphine (Scheme 1). The olefinic substrate, being more π-accepting, binds to coordinatively unsaturated complex **4** much more effectively than any free phosphine present in solution. Thus, it is actually k_2/k_{-1} rather than just k_1 that determines how much of the Ru complex actually enters the catalytic cycle. Piers et al. [6,7] have recently developed another NHC Ru complex (**3**, Chart 1) that has a phosphonium salt on the initial alkylidene ligand, and is already highly coordinatively unsaturated (14 electron). Since **3** has no phosphine *trans* to the carbene that needs to dissociate prior to binding of the

* Corresponding author.
E-mail address: cruddenc@chem.queensu.ca (C.M. Crudden).
[1] Author to whom correspondence concerning X-ray crystallography should be addressed.

0022-328X/$ - see front matter © 2005 Published by Elsevier B.V.
doi:10.1016/j.jorganchem.2005.07.037

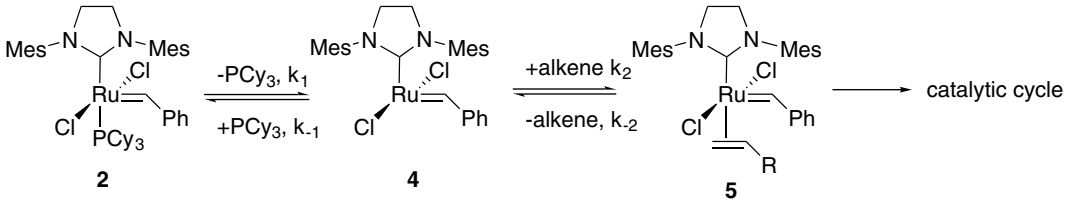

Scheme 1. Initiation of Grubbs II catalyst.

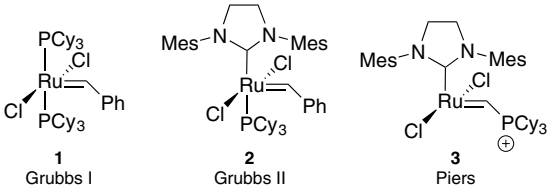

Mes = 2, 4, 6 trimethylbenzene

Chart 1. Recent Ru-based metathesis catalysts.

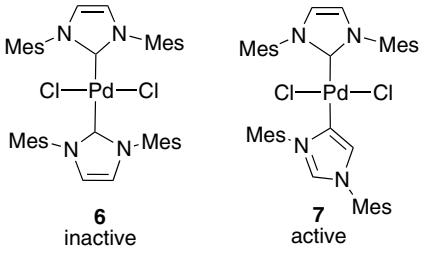

Chart 2. *N*-heterocyclic carbene complexes of Pd prepared by in situ routes.

alkene, it displays very high activity in the metathesis reaction.

In addition to olefin metathesis, coupling reactions like the Mizoroki-Heck and Suzuki-Miyaura reactions were among the first reactions to be attempted with *N*-heterocyclic carbene complexes [8]. The effectiveness of the NHC-containing catalysts were assumed to be due to the more electron donating carbene ligand, which leads to a more electron rich complex, favouring oxidative addition. However, Lebel and co-workers [9] have shown that the method of preparation of the NHC–Pd complex has a significant effect on the exact nature of the catalyst that is generated. During an attempted preparation of $X_2Pd(IMes)_2$(IMes = 1,3 dimesitylimidazol-2-ylidene) as a precursor to the catalytically active $Pd(IMes)_2$ species, $Pd(OAc)_2$ was treated with two equivalents of IMesHCl in dioxane at 60 °C. Although this preparation is commonly employed for the in situ generation of carbene complexes, it does not lead to the expected complex. Instead Lebel isolates the $Pd(NHC)_2Cl_2$ complex resulting from metalation on the backbone of the carbene (**7**). This complex has high catalytic activity in the Heck reaction, while the desired complex **6**, prepared under different conditions, was completely inactive, which emphasizes the importance of using isolated complexes rather than in situ procedures which may produce different complexes [10]. In this case, it is postulated that the initially formed mono-ligated carbene complex predisposes the Pd towards oxidative addition into the backbone of the second imidazolium salt, leading to **7** (see Chart 2).

Our lab has also demonstrated that instability of the carbene–Rh bond can lead to the generation of new, non-carbene containing species with high catalytic activity [11]. As part of a study of the behaviour of NHC analogs of Wilkinson's catalyst, we examined the catalytic activity and phosphine exchange kinetics of Rh complex **8a**. Consistent with the effect observed by Grubbs in the Ru alkylidene series, we found that the NHC ligand dramatically decreased the rate of exchange of the *trans* phosphine, relative to the all phosphine containing complex (Wilkinson's complex) [11]. While examining different solvents, we found that halogenated solvents such as dichloroethane and dichloromethane promoted the conversion of **8a** and its congeners into Wilkinson's complex (**9**) in the presence of added triaryl phosphine (Eq. (1)). The displaced carbene ligand yielded the bisimidazolium salt **10** resulting from reaction with solvent. Although the precise mechanism of this reaction is not clear, an identical product distribution is obtained when the free carbene **(12)** is treated with $ClCH_2CH_2Cl$ at 80 °C. These results are significant since Wilkinson's catalyst is more active than **8** in hydrogenation reactions, so inadvertent loss of the carbene will lead to a *more* active catalyst. Indeed we showed that the addition of dichloroethane to a reaction run in THF led to a rate acceleration, even under conditions where only small amounts of **8** would be converted into **9**.

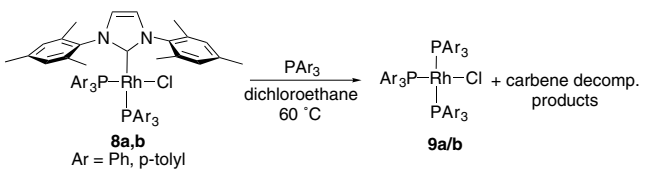

(1)

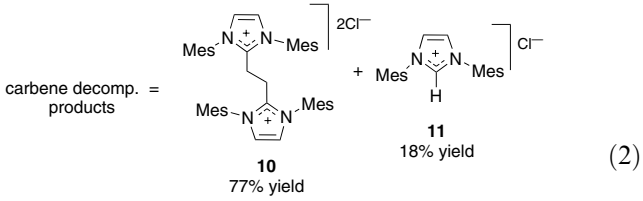

(2)

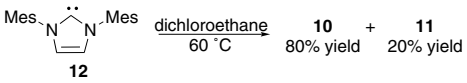

Remarkably, the related carbonyl complex [Rh(IMes)(PAr_3)(CO)Cl] is completely stable under these conditions showing no sign of decomposition even after 16 h in dichloroethane at 80 °C. This might be attributed to the ability of the carbonyl ligand to withdraw electron density from the already very electron rich Rh complex, stabilizing it toward loss of the carbene. Steric hindrance also likely plays a role since the steric bulk of the carbene ligand causes the phosphines to be disposed in a *cis* fashion in the complex *cis* phosphine, which distorts the complex from the ideal square planar geometry. The carbonyl complex is nearly perfectly square planar [12].

We report herein the structure, catalytic activity and phosphine dissociation rates for several phosphine analogs of the bis triaryl phosphines **8a** and **b** in an attempt to gauge the factors affecting phosphine dissociation and catalytic activity.

2. Results and discussion

2.1. Synthesis and characterization of Rh NHC complexes

Rhodium-*N*-heterocyclic carbene complexes **8a–f** were prepared by treatment of the corresponding [$RhCl(PR_3)_3$] complex with one equivalent of free IMes (**12**) Eq. (3). Phosphite complex **8f** could be prepared by this method in 52% yield, but higher yield (70%) was obtained by treatment of all [$Rh(CH_2{=}CH_2)_2Cl]_2$ with $P(OPh)_3$ and free carbene. The advantage of this route is that there are no byproducts since the carbene was pregenerated, and the dimer is cleaved without loss of another ligand Eq. (4).

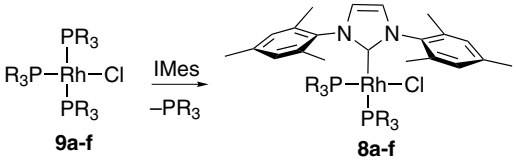

(3)

a, PPh_3, **b**, $P(p\text{-}MeC_6H_4)_3$
c, $P(p\text{-}MeOC_6H_4)_3$, **d**, $P(p\text{-}FC_6H_4)_3$
e, $P(2\text{-furyl})_3$, **f**, $P(OPh)_3$

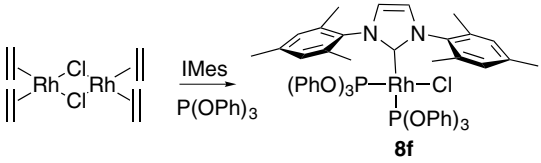

(4)

As previously noted, [$ClRh(PAr_3)_2L$] type complexes generally prefer to have the two phosphines positioned *trans* to one another to decrease steric hindrance. However, the extreme steric bulk of the IMes ligand forces these two substituents to occupy *cis* positions around Rh [13], introducing considerable strain into the complex, as evidenced by the distortions from planarity and from distortions the ideal 90° geometry about the complex revealed in the X-ray crystallographic structures (Figs. 1–4, Tables 1 and 2).

As shown in Table 1, the more electron rich the phosphine is, the longer the rhodium–NHC carbon bond is, ranging from 2.0574(18) Å for the trifuryl complex **8e**, to 2.045(2) for the *p*-fluoro phosphine complex **8d**. In addition, there is a slight elongation of the PC bonds to the aryl carbon in the case of the *trans* phosphines relative to the *cis* phosphines as the complex becomes more electron rich, implying greater backbonding to the phosphine. However, the effect is not pronounced, and there are some large deviations in individual aryl rings (last entries for **8c** and **8d**) which are likely due to packing effects.

Solution-phase characterization of the complexes indicated that the phosphines were disposed in a *cis* orientation by the presence of two phosphine signals, both doublets of doublets because of coupling to each other and to the NMR active spin 1/2 Rh nucleus. However, the ^{31}P NMR spectra of complexes **8e** and **8f** are quite

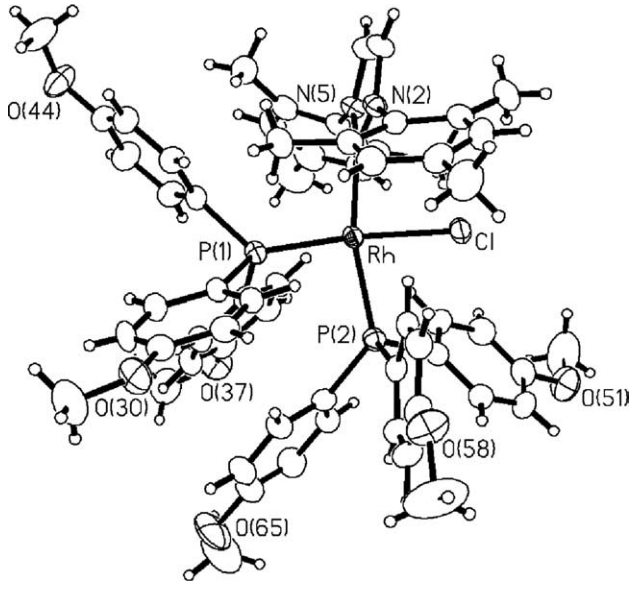

Fig. 1. ORTEP diagram of [(IMes)Rh($P(p\text{-}OMe\text{-}Ph)_3)_2Cl$] (**8c**) with ellipsoids drawn at 50% probability.

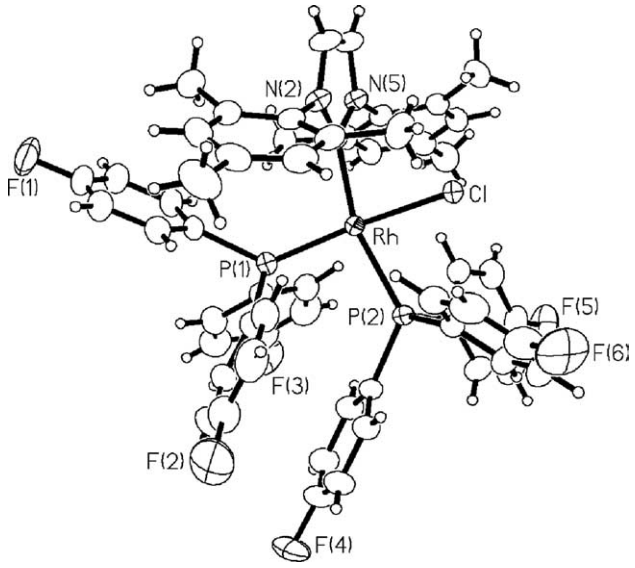

Fig. 2. ORTEP diagram of [(IMes)Rh(P(*p*-F-Ph)$_3$)$_2$Cl] (**8d**) with ellipsoids drawn at 50% probability.

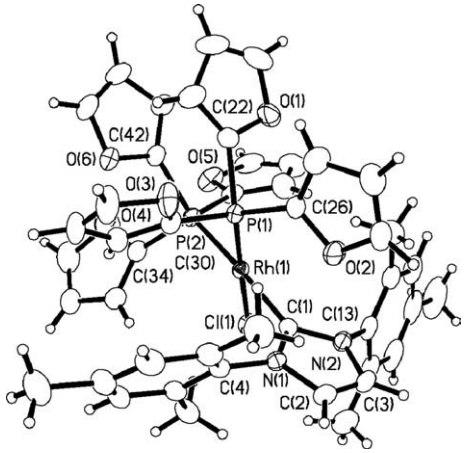

Fig. 3. ORTEP diagram of [(IMes)Rh(P(2-furyl)$_3$)$_2$Cl] (**8e**) with ellipsoids drawn at 50% probability.

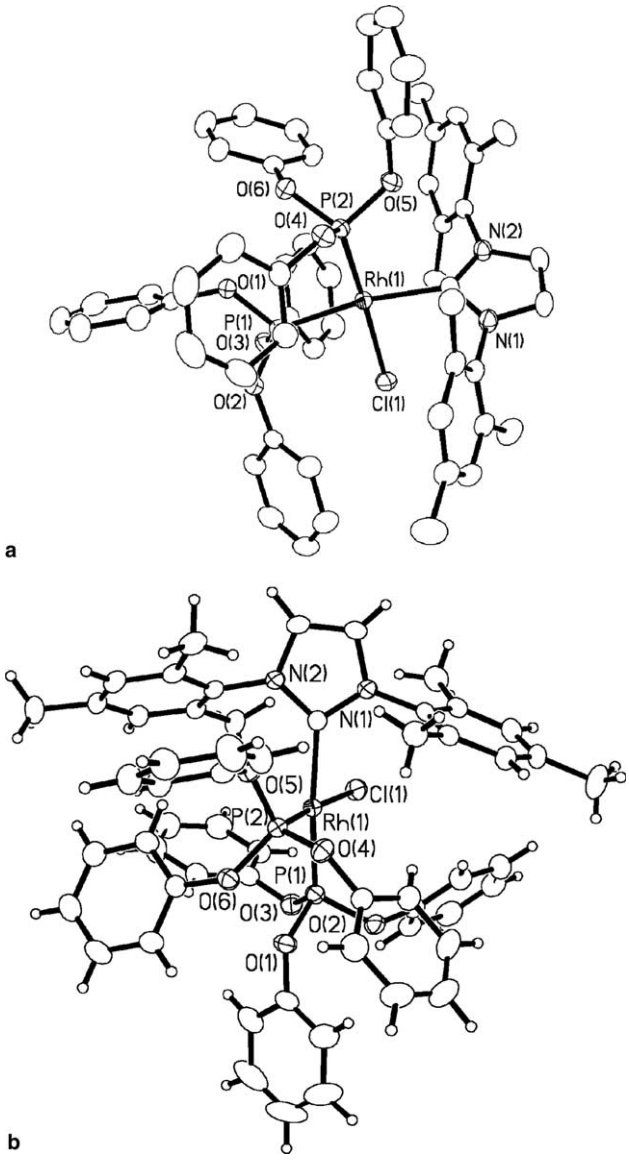

Fig. 4. (a) ORTEP diagram of [(IMes)Rh(P(OPh)$_3$)$_2$Cl] (**8f**) with ellipsoids drawn at 50% probability. (b) ORTEP diagram of [(IMes)Rh(P(OPh)$_3$)$_2$Cl] (**8f**) (second orientation of the molecule) with ellipsoids drawn at 50% probability.

complex and variable depending on the solvent employed. Spin simulations performed on the ABX system were carried out to reveal the chemical shifts and coupling constants as shown in Fig. 5 for the spectrum of **8f** performed in benzene and in Fig. 6 for **8f** in THF.

2.2. Catalytic studies

The hydrogenation of *E*-β-methyl styrene (**13**) was examined employing carbene complexes **8a**–**f** in THF (Eq. (4)). Previous studies indicated that catalyst **8a** was essentially unreactive at room temperature due to the lack of phosphine dissociation, which is the first step in hydrogenations with Wilkinson's type complexes [15,16]. Only after heating to 60 °C, at which temperature phosphine dissociation takes place at a rate of ca. 1/s, does the reaction begin. The addition of CuCl, a known phosphine sponge [17], increases the catalytic activity significantly, implying that phosphine dissociation is critical for the activity of the NHC complexes as well [11]. In the presence of CuCl, complex **8a** was shown to be active even at room temperature. At 60 °C, the activity of **8a** for the hydrogenation of isosafrole even exceeded that of Wilkinson's catalyst (**9a**, compare entries 2 and 8, as well as 1 and 7, Table 3).

The NHC–Rh complexes examined had similar rates of reaction for the hydrogenation of β-methylstyrene with the exception of triphenyl phosphite complex **8f**, which is virtually inactive, even in the presence of CuCl

Table 1
Selected bond lengths (Å) and angles (°) for **8a**–**f**

	8a [14]	**8c**	**8d**	**8e**	**8f**
Bond lengths					
Rh–C_{NHC}	2.0527(14)	2.056(3)	2.045(2)	2.0574(18)	2.0851(15)
Rh–P_{cis}	2.2158(4)	2.2232(8)	2.2145(6)	2.1722(6)	2.1452(5)
Rh–P_{trans}	2.3053(4)	2.3263(9)	2.3284(5)	2.2803(6)	2.2147(5)
Rh–Cl	2.3941(4)	2.4012(7)	2.3752(5)	2.3951(6)	2.3761(5)
P_{trans}–C_{aryl}	–	1.850(3)	1.838(2)	1.8023(19)	1.6108(12)[a]
P_{trans}–C_{aryl}	–	1.845(3)	1.839(2)	1.814(2)	1.6162(12) [a]
P_{trans}–C_{aryl}	–	1.843(3)	1.849(2)	1.8264(19)	1.6175(12)[a]
P_{cis}–C_{aryl}	–	1.834(3)	1.841(3)	1.799(2)	1.6153(11)[a]
P_{cis}–C_{aryl}	–	1.841(3)	1.842(3)	1.811(2)	1.6256(11)[a]
P_{cis}–C_{aryl}	–	1.859(3)	1.867(2)	1.816(2)	1.6302(12)[a]
Bond angles					
C_{NHC}–Rh–P_{trans}	164.10(4)	165.49(8)	162.48(6)	172.47(5)	169.58(4)
C_{NHC}–Rh–P_{cis}	98.43(4)	101.71(8)	102.29(6)	92.01(5)	93.54(4)
P–Rh–P	96.238(15)	92.79(3)	95.12(2)	95.527(19)	96.838(17)
Cl–Rh–P_{cis}	173.835(15)	173.87(3)	175.77(2)	177.995(18)	174.829(16)
Cl–Rh–P_{trans}	80.187(13)	81.34(3)	80.731(19)	83.502(18)	82.220(16)

[a] P–O bonds instead of P–C bonds are listed in the case of **8e**.

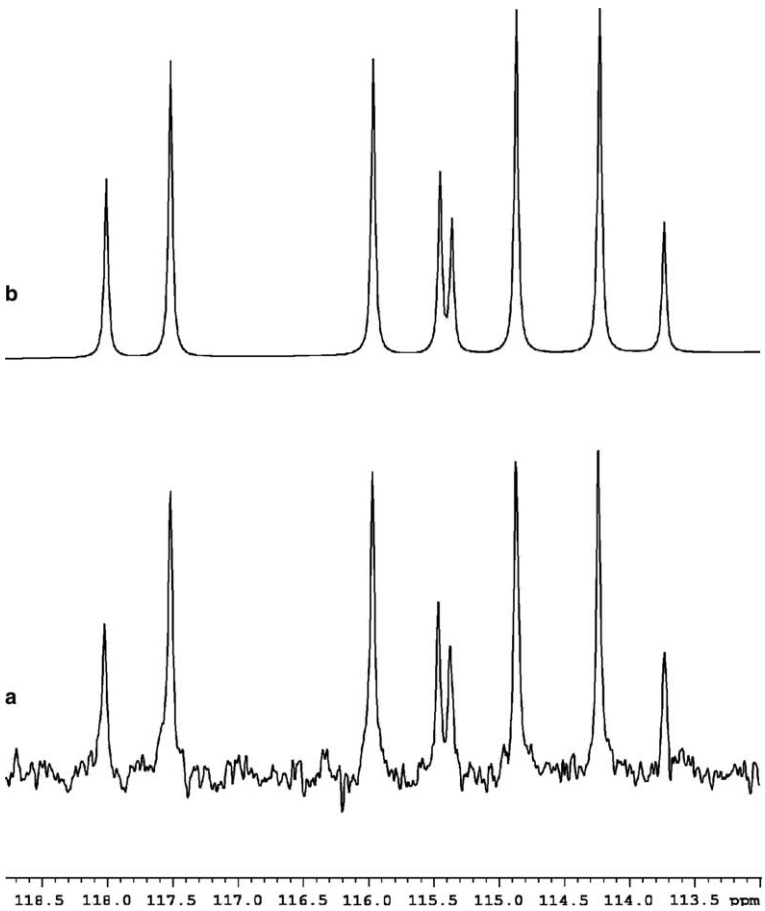

Fig. 5. Experimental ^{31}P NMR spectrum (a), recorded in benzene-d_6, comprising the AB portion of the ^{31}P, ^{31}P, ^{31}Rh ABX spin system of rhodium carbene complex **8f**. The simulated spectrum (b), was obtained by iterative variation of the parameters δA, δB, JAB, JAX, and JBX resulting in an RMSD of 0.02 Hz between the simulated and experimental spectra. The fitted chemical shifts and coupling constants were $\delta A = 114.9$ ppm, $\delta B = 116.4$ ppm, JAB = 62 Hz, JAX = 208 Hz, and JBX = 327 Hz. The simulation was performed using the spin simulation module of Varian, Inc. VNMR 6.1C software.

Table 2
Crystallographic data and structure refinement for **8c–f**

Empirical formula	$C_{63}H_{68}ClN_2O_6P_2Rh \cdot THF$ (**8c**)	$C_{57}H_{48}ClF_6N_2P_2Rh \cdot 1/2C_6H_{14}$ (**8d**)	$C_{45}H_{42}N_2O_6P_2ClRh$ (**8e**)	$C_{57}H_{54}ClN_2O6P_2Rh$ (**8f**)
Formula weight	1219.58	1118.36	907.11	1135.43
Crystal system	Monoclinic	Monoclinic	Triclinic	Triclinic
Space group	$P2_1c$	$P2_1/c$	$P1$	$P1$
Unit cell dimensions				
a (Å)	15.6874(15)	11.5245(6)	11.4356(18)	11.0592(18)
b (Å)	15.4397(15)	33.507(2)	11.8006(18)	12.1444(19)
c (Å)	25.696(2)	14.1727(8)	15.571(2)	22.777(4)
α (°)	90	90	84.504(3)	86.345(3)
β (°)	90.146(2)	105.695(1)	89.824(3)	77.624(3)
γ (°)	90	90	83.312(3)	65.245(3)
Volume (Å^3)	6223.8(10)	5268.7(5)	7291(2)	2712.3(8)
Z	4	4	2	4
Density (calc) (Mg/m^3)	1.302	1.410	1.450	1.390
Crystal size (mm^3)	$0.75 \times 0.225 \times 0.325$	$0.125 \times 0.225 \times 0.375$	$0.35 \times 0.15 \times 0.15$	$0.4 \times 0.4 \times 0.3$
$F(000)$	2552	2300	932	1180
Reflections collected	30446	36555	14806	19175
Independent reflections	10504[$R_{int} = 0.0417$]	11743[$R_{int} = 0.0243$]	9382[$R_{int} = 0.0135$]	12142[$R_{int} = 0.0121$]
Data/restraints/parameters	10504/4/987	11743/0/841	9382/0/682	13557/0/603
Final R indices [$I > 2\sigma(I)$]	$R_1 = 0.0406$, $wR_2 = 0.0915$	$R_1 = 0.0352$, $wR_2 = 0.0880$	$R_1 = 0.0281$, $wR_2 = 0.0649$	$R_1 = 0.0269$, $wR_2 = 0.0697$
R indices (all data)	$R_1 = 0.0703$, $wR_2 = 0.0999$	$R_1 = 0.0446$, $wR_2 = 0.0918$	$R_1 = 0.0354$, $wR_2 = 0.0685$	$R_1 = 0.0335$, $wR_2 = 0.0723$
Goodness-of-fit on F^2	1.048	1.069	1.025	1.031
Theta range for data collection (°)	1.54–24.99	1.61–27.50	1.31–28.33	1.83–28.31
Absorption coefficient (mm^{-1})	0.422	0.498	0.603	0.479
Largest difference in peak and hole (e Å^{-3})	1.055 and −0.537	0.636 and −0.530	0.620 and −0.225	0.872 and −0.304

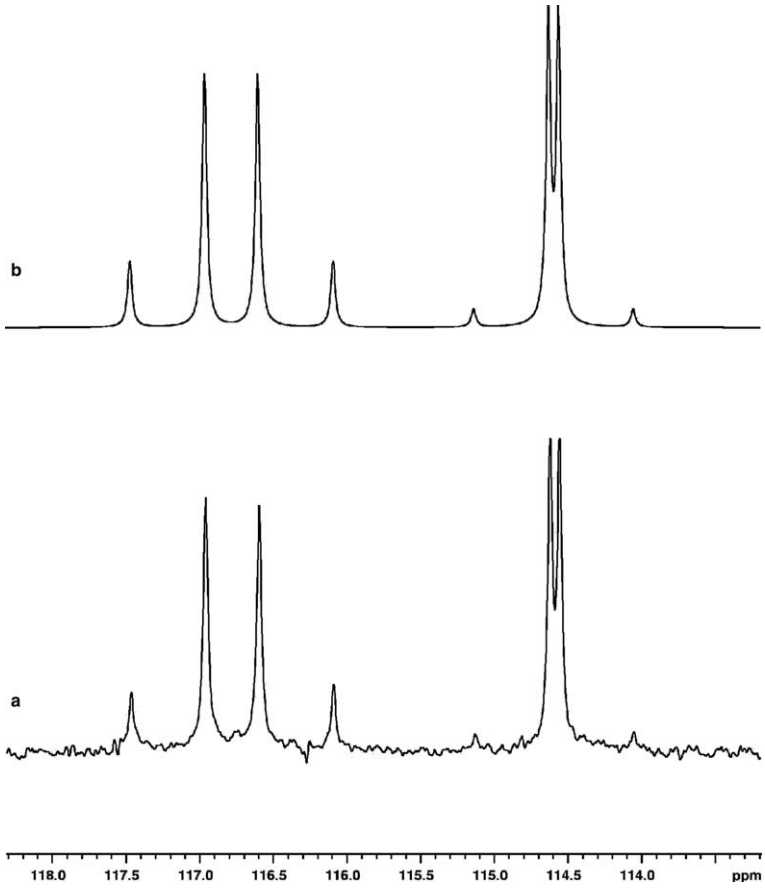

Fig. 6. Experimental ^{31}P NMR spectrum (a), recorded in tetrahydrofuran-d_8, comprising the AB portion of the ^{31}P, ^{31}P,^{103}Rh ABX spin system of rhodium carbene complex **8f**. The simulated spectrum (b), was obtained by iterative variation of the parameters δA, δB, JAB, JAX, and JBX resulting in an RMSD of 0.2 Hz between the simulated and experimental spectra. The fitted chemical shifts and coupling constants were $\delta A = 115.6$ ppm, $\delta B = 115.8$ ppm, JAB = 62 Hz, JAX = 207 Hz, and JBX = 326 Hz. The simulation was performed using the spin simulation module of Varian, Inc. VNMR 6.1C software.

or BPh_3. Of all the NHC–Rh complexes examined, the *p*-fluoro derivative **8d** was found to have the highest inherent activity, approximately twice that of the triphenyl phosphine derivative **8a** (compare entries 1 and 4). Interestingly, *p*-fluoro derivative **8d** has a muted response to CuCl. Complexes **8a** and **8c** are accelerated by factors of 14 and 83, respectively, but **8d** is only 3.7 times faster in the presence of CuCl.

Although triphenyl boron was also examined as a phosphine scavenger, it was generally not as effective, even at 2.5 equivalents (second entry). The triphenylphosphite derivative **8f** displayed very little activity even after treatment with CuCl or BPh_3.

To examine the effect of solvent on the reaction, we also tested the activity of a few of the complexes in toluene and noticed a significant decrease in activity (Table 4). The inherent activity was much lower in toluene, with complex **8a** showing the largest decrease of almost a factor of ten. Both the *p*-methoxy and the *p*-fluoro derivatives have approximately half the activity in toluene compared with THF. Again, the addition of CuCl increases the rate of reaction, but less so than it does in THF.

Since compound **8d** has high inherent activity in the absence of CuCl which is not increased dramatically upon addition of CuCl, we decided to examine the phosphine dissociation of this complex. Remarkably, the rate of phosphine dissociation was actually slower than the *p*-tolyl derivative **8b**, which is a good model for the PPh_3 derivative **8a** [18]. At 50 °C, the rate of exchange of the *p*-fluoro complex **8d** was only 0.07 s^{-1}, compared with 0.35 s^{-1} for **8b**. At higher temperatures the trend continued with **8b** always having a higher rate of exchange than **8d**. The rate of exchange in the case of **8d** is independent of solvent, occurring at virtually equal rates in either toluene or THF (see Table 5). It may be that the higher inherent activity of **8d** renders phosphine dissociation less important to the catalytic activity of this complex, but the dissociation rates of more of the NHC complexes need to be determined before a definitive statement can be made [19]. These studies are currently underway.

Table 3
Hydrogenation activity of catalysts **8a–f** and **9a**, and the effect of additives[a]

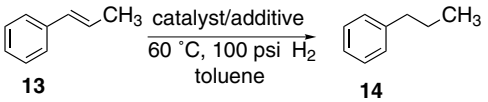

13 **14** (5)

Entry	Catalyst (phosphine)	TOF (h^{-1}) and additive effects[b]		
		None	CuCl[c]	BPh_3[d]
1	**8a**, PPh_3	24	331	17, 32
2	**8a**, PPh_3[e]	50	430	–
3	**8c**, P(*p*-$MeOC_6H_4)_3$	5	417[f]	7, 12
4	**8d**, P(*p*-$FC_6H_4)_3$	43	161	38, 90
5	**8e**, P(2-furyl)$_3$	9	24	–
6	**8f**, P(OPh)$_3$	0.25	0.4	0.2, 0.8
7	**9a** (PPh_3)	297	243	276, 268
8	**9a** (PPh_3)[e]	250	300	–

[a] Reactions were carried out in an autoclave, under 100 psi of H_2, with 0.75% catalyst, $[substrate]_{init} = 0.1$ M in dry, deoxygenated, distilled THF at 60 °C. Solutions were prepared in a glove box under argon.
[b] Turnover frequency per hour, measured after 15 min.
[c] One equivalent.
[d] TOF with 1.0 or 2.5 equiv., respectively.
[e] 3,4-Methylenedioxy β-methylstyrene was employed as the substrate at 200 psi of H_2.
[f] Reaction was 97% complete after 15 min so the TOF listed is probably an underestimate.

Table 4
Hydrogenation activity of catalysts **8a–d**, in toluene[a]

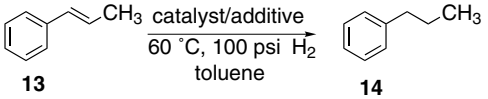

13 **14** (5)

Entry	Catalyst (phosphine)	TOF (h^{-1})[b]	
		None	CuCl[c]
1	**8a**, PPh_3	3.5	188
2	**8c**, P(*p*-$MeOC_6H_4)_3$	2.3	190
3	**8d**, P(*p*-$FC_6H_4)_3$	24	123

[a] See footnote to Table 4, except the reaction was run in toluene.
[b] Turnover frequency per hour, measured after 30 min.
[c] One equivalent.

Table 5
Rates of phosphine exchange in Rh complexes **8b** and **8d**[a]

Entry	Complex	Solvent	Exchange rate (s^{-1})			
			50 °C	60 °C	70 °C	80 °C
1	**8b** (P(*p*-$CH_3C_6H_4)_3$)	Toluene	0.35	0.91	2.4	n.d[b]
2	**8d** (P(*p*-$FC_6H_4)_3$)	Toluene	0.07	0.26	0.79	2.25
3	**8d** (P(*p*-$FC_6H_4)_3$)	THF	0.07	0.20	n.d[b]	n.d[b]

[a] Exchange experiments carried out at the indicated temperature in dry distilled solvent, $\mathbf{8} = 0.04$ M using a delay time at least $= 5 \times T_1$. Solutions were prepared in a glove box under argon and are in sealed tubes or NMR tubes fitted with J-Young valves. See experimental for full details.
[b] Not determined.

3. Conclusions

In conclusion, we have demonstrated that IMes ligated complexes **8a–f** are effective catalysts for the hydrogenation of olefins, with increases of almost two orders of magnitude observed in the rate of hydrogenation in the presence of CuCl. Interestingly the *p*-fluoro derivative seems to have a high inherent hydrogenation ability and little response to CuCl despite the fact that the phosphine dissociation rate is relatively slow.

4. Experimental

4.1. General considerations

All the reactions were carried out in a dry Argon or nitrogen atmosphere using standard Schlenk techniques or in a Mbraun glovebox (nitrogen) containing less than 1 ppm of oxygen and water. NMR spectra were recorded using Varian Unity 400, Bruker 300, 400 or 500 MHz spectrometers. All reported TOF's were determined by gas chromatography using decane as an internal standard.

4.2. Reagents

All solvents were purified by standard procedure and degassed prior to use by 3 freeze/pump/thaw cycles. β-Methyl styrene was purchased from commercial suppliers and distilled and degassed (3 × fpt) and stored cold in the glovebox. It was passed through a plug of activated basic alumina before each hydrogenation experiment. Wilkinson's catalyst was purchased commercially and used as received. IMesHCl [20], IMes [20], RhCl((P-*p*-tolyl)$_3)_3$ [21] were prepared according to the literature procedures.

4.3. Preparation of [(IMes)Rh(P(p-OMe-Ph)$_3)_2$Cl] (8c)

An oven dried 50 ml schlenk flask with stir bar was taken into the glovebox and was charged with [Rh(P(*p*-OMe-Ph)$_3)_3$Cl] (317 mg, 0.265 mmol). Then, IMes (85 mg, 0.280 mmol) was added to the schlenk flask. Then dry, deoxygenated toluene (15 ml) was added and the resulting dark orange homogeneous solution gradually lightened in color to an orange-yellow solution after stirring for 22 h. At this stage, the sealed schlenk flask was removed from the glovebox and placed on the schlenk line where the solution was concentrated to a volume of approximately 2 ml. Then dry, deoxygenated hexane (15 ml) was added to precipitate a fine, yellow solid. This mixture was cooled at −20 °C for 2 h, and then filtered using a schlenk apparatus. The solid was washed with hexane (3 × 10 ml) and

then dried under vacuum overnight to yield a light yellow solid (302 mg, 99%). X-ray quality crystals were obtained via slow vapour diffusion of hexane into a THF solution of the rhodium complex.

^{1}H NMR (400 MHz, C_6D_6), δ:

1.92 (s, 6H), 2.42 (s, 6H), 2.91 (s, 6H), 3.26 (s, 9H), 3.29 (s, 9H), 6.37 (s, 2H), 6.57 (m,12H), 6.91 (s, 2H), 7.15 (s, 2H), 7.75–7.25 (br, 12H)

^{13}C NMR (600 MHz, C_6D_6), δ:

20.29, 21.42, 22.39, 54.61, 54.67, 112.39, 112.50, 112.59, 122.93, 127.95, 128.67,130.02, 130.43, 135.81, 136.70 (m), 137.45, 137.62 (d, $J = 11.2$ Hz), 138.74, 139.32,160.01 (d, $J = 44$ Hz), 191.5 (ddd, $J = 117$, 49, 14 Hz)

^{31}P NMR (400 MHz, d_8-toluene), δ:

44.95 (dd, $J_{P-Rh} = 207$ Hz, $J_{P-P} = 40$ Hz), 32.60 (dd, $J_{P-Rh} = 121$ Hz, $J_{P-P} = 40$ Hz)

MS (*m*/*z*)

$[M - Cl]^+ = 1111.3058$, 1112.3114, 1113.3079, 1114.3009 (calculated isotope distribution = 1111.4, 1112.4, 1113.4, 1114.4).

4.4. Preparation of [(IMes)Rh(P(p-F-Ph)$_3$)$_2$Cl] (**8d**)

An oven dried 50 ml schlenk flask with stir bar was taken into the glovebox, and was charged with [Rh(P(*p*-F-Ph)$_3$)$_3$Cl] (251 mg, 0.231 mmol). Then IMes (76 mg, 0.250 mmol) was added to the schlenk flask. Then dry, deoxygenated toluene (15 ml) was added and the light orange mixture turned homogeneous and gradually lightened to a pale yellow solution after stirring for 16 h. At this stage, the sealed schlenk flask was removed from the glovebox and placed on the schlenk line where the solution was concentrated to a volume of approximately 2 ml. Then dry, deoxygenated hexane (15 ml) was added to precipitate a fine, light yellow solid. This mixture was cooled at −20 °C for 2 h, and then filtered using a schlenk apparatus. The solid was washed with hexane (3 × 10 ml) and then dried under vacuum overnight to yield a light yellow solid (243 mg, 98%).

^{1}H NMR (400 MHz, C_6D_6), δ:

1.58 (s, 6H), 2.32 (s, 6H), 2.70 (s, 6H), 6.23, (s, 2H), 6.54 (m, 12H), 6.69 (s, 2H), 7.01 (s, 2H), 7.45–7.02 (br, 12H)

^{13}C NMR (400 MHz, C_6D_6), δ:

20.14, 21.51, 22.20, 114.42 (m), 123.46, 128.93, 130.34, 133.21, 133.60, 135.73, 137.08 (br), 138.06 (m), 138.33, 138.44, 139.31, 162.45 (d, $J = 29$ Hz), 164.95 (d, $J = 30$ Hz), 188.50 (ddd, $J = 117$, 49, 14 Hz)

^{31}P NMR (400 MHz, d_8-toluene), δ:

46.24 (dd, $J_{P-Rh} = 208$ Hz, $J_{P-P} = 39$ Hz), 33.66 (dd, $J_{P-Rh} = 121$ Hz, $J_{P-P} = 39$ Hz).

4.5. Preparation of [(IMes)Rh(P(2-furyl)$_3$)$_2$Cl] (**8e**)

An oven dried 50 ml schlenk flask with stir bar was taken into the glovebox, charged with $[Rh(C_2H_4)_2Cl]_2$ (102.36 mg, 0.263 mmol) and dissolved in dry, deoxygenated toluene (7 ml). In a separate vial, P(2-furyl)$_3$ (242.46 mg, 1.04 mmol) was diluted with toluene (3 ml). The phosphine solution was then added to the schlenk flask containing the rhodium complex and this was stirred for 30 min. At this stage, the rhodium/phosphine solution was gravity filtered into a 50 ml schlenk flask containing an IMes (156 mg, 0.512 mmol) solution in toluene (3 ml). A further 2 ml of toluene was used to rinse the filter paper. This mixture was then stirred for 16 h. At this stage, the sealed schlenk flask was removed from the glovebox and placed on the schlenk line where the solution was concentrated to a volume of approximately 2 ml. Then dry, deoxygenated hexane (15 ml) was added to precipitate a fine yellow solid. This mixture was cooled at −20 °C for 2 h, and then filtered using a schlenk apparatus. The solid was washed with hexane (3 × 10 ml) and then dried under vacuum overnight to yield a light yellow solid (442.83 mg, 93%). X-ray quality crystals were obtained via slow vapour diffusion of hexane into a THF solution of the rhodium complex.

^{1}H NMR (500 MHz, C_6D_6), δ:

2.01 (s, 6H), 2.23 (s, 6H), 2.82 (s, 6H), 5.89 (m, 3H), 5.98 (m, 3H), 6.43 (s, 2H), 6.59 (br, 3H), 6.79 (br, 5H), 6.95 (br, 2H) 6.99 (m, 6H)

^{13}C NMR (500 MHz, C_6D_6), δ:

19.5, 21.4, 22.0, 110.6 (d, $J = 6.8$ Hz), 111.1 (d, $J = 7.2$ Hz), 122.5 (d, $J = 20.6$ Hz),123.4, 123.6 (d, $J = 19.2$ Hz), 129.2, 130.2, 135.7, 137.9, 138.4, 139.2, 145.4 (d, $J = 4.2$ Hz), 146.0 (d, $J = 3.9$ Hz), 148.8 (d, $J = 56.7$ Hz), 151.0 (d, $J = 56.6$ Hz)

^{31}P NMR (500 MHz, C_6D_6), δ:

−8.6 (dd, $J_{P-Rh} = 206$ Hz, $J_{P-P} = 44$ Hz), 7.8 ppm, (dd, $J_{P-Rh} = 123$ Hz, $J_{P-P} = 44$ Hz).

4.6. Preparation of [(IMes)Rh(P(OPh)$_3$)$_2$Cl] (**8f**)

Route 1: an oven dried 50 ml schlenk flask with stir bar was taken into the glovebox and charged with [Rh(P(OPh)$_3$)$_3$Cl] (148 mg, 0.139 mmol). Then, IMes (46.0 mg, 0.150 mmol) was weighed and added to the schlenk flask. Then dry, deoxygenated toluene (10 ml) was added and the yellow mixture turned homogeneous and gradually lightened to a very pale yellow solution after stirring for 16 h. At this stage, the sealed schlenk flask was removed from the glovebox and placed on the schlenk line where the solution was concentrated to a volume of approximately 1 ml. Then dry, deoxygenated hexane (8 ml) was added to precipitate a fine, light yellow solid. This mixture was cooled at −20 °C for 2 h, and then filtered using a schlenk apparatus. The solid was washed with hexane (3 × 5 ml) and then dried under vacuum overnight to yield a light yellow solid (75.6 mg, 52%).

Route 2: an oven dried 50 ml schlenk flask with stir bar was taken into the glovebox. $[Rh(C_2H_4)_2Cl]_2$

(99 mg, 0.254 mmol) was weighed and dissolved in dry, deoxygenated toluene (7 ml). In a separate vial, $P(OPh)_3$ (315 mg, 1.01 mmol) was weighed and then diluted with toluene (3 ml). The phosphite solution was then added to the schlenk flask containing the rhodium complex and this was stirred for 30 min. At this stage, the rhodium/phosphite solution was gravity filtered into a 50 ml schlenk flask containing an IMes (156 mg, 0.512 mmol) solution in toluene (3 ml). A further 2 ml of toluene was used to rinse the filter paper. This mixture was then stirred for 16 h. At this stage, the sealed schlenk flask was removed from the glovebox and placed on the schlenk line where the solution was concentrated to a volume of approximately 2 ml. Then dry, deoxygenated hexane (15 ml) was added to precipitate a fine, light yellow solid. This mixture was cooled at −20 °C for 2 h, and then filtered using a schlenk apparatus. The solid was washed with hexane (3 × 10 ml) and then dried under vacuum overnight to yield a light yellow solid (376 mg, 70%). X-ray quality crystals were obtained from slow vapour diffusion of hexane into a THF solution of the rhodium complex.

^{1}H NMR (400 MHz, C_6D_6), δ:

2.24 (s, 6H), 2.33 (s, 6H), 2.47 (s, 6H), 6.26 (s, 2H), 6.76–6.80 (br, 5H), 6.84–6.91 (m, 8H), 6.94–7.03 (m, 15H), 7.05–7.95 (br, 6H)

^{13}C NMR (600 MHz, C_6D_6), δ:

19.4, 21.1, 21.3, 122.2 (d, $J = 4.3$ Hz), 122.6 (d, $J = 4.1$ Hz), 123.5, 123.7, 128.3, 128.8,128.9, 129.3, 130.0, 136.3, 137.7, 138.2, 138.4, 152.4 (d, $J = 8.7$ Hz), 152.7 (d, $J = 8.2$ Hz), 187.5 (ddd, $J = 184$, 48, 14 Hz)

^{31}P NMR (400 MHz, C_6D_6), δ:

114.9 (dd, $J_{P-Rh} = 208$ Hz, $J_{P-P} = 62$ Hz), 116.4 ppm, (dd, $J_{P-Rh} = 327$ Hz, $J_{P-P} = 62$ Hz).

MS (*m*/*z*):

$[M - Cl]^+ = 1027.2653$, 1028.2694, 1029.2624, 1030.2666 (calculated isotope distribution = 1027.3, 1028.3, 1029.3, 1030.3).

4.7. Typical hydrogenation reaction

The Rh catalyst (**8** or **9**) (0.01 mmol) and β-methylstyrene (1.3 mmol) were loaded into a glassliner and dissolved in 7 ml of THF. This was then placed in a high pressure autoclave and assembled. The autoclave was filled and flushed three times with H_2 before it was finally pressurized to 100 psi. The autoclave was then allowed to stir for 30 min (either at r.t. or 60 °C). At this time, the pressure was released and the autoclave was disassembled. All the contents were then transferred to a vial containing a known amount of decane as an internal standard. The resulting mixture was analyzed by gas chromatography to determine the % conversion and subsequent TOF.

4.8. Typical NMR experiment for determination of exchange rate

NMR samples were prepared inside a nitrogen filled glove box using tubes fitted with J-Young valves, or in flame sealed tubes. Rh complex **8d** was added into the NMR tube (0.03 mmoles) along with excess phosphine (3 equiv.), and 0.75 mL of solvent. The T_1's of the isolated phosphine and the phosphine in the presence of the Rh complex were measured at room temperature using the standard inversion recovery method, and a relaxation delay time of $5 \times T_1$ for the largest T_1 was employed for the inversion transfer experiments. The temperature was raised to the desired point, and allowed to equilibrate with the sample in the probe for 15 min before beginning the experiment.

The ^{31}P inversion transfer experiments were performed as follows: a 180° selective pulse was applied to the signal for free phosphine with the transmitter on resonance. Delay times of 0 s to $5 \times T_1$ were applied in increments followed by a 90° read pulse. The data were acquired successively in blocks of 4 transients at each delay time. The free-induction decays were zero-filled prior to Fourier transformation and a baseline correction routine was applied to the resulting spectra prior to integration of the phosphine signals. The exchange rate of bound and free phosphine was extracted by fitting the integration of these signals at increasing delay times to a two-site exchange model using either Bain's CIFIT program [22], or a programmable spreadsheet. Error analysis of the calculated exchange rates was performed using the method of Bain and Cramer [22] to yield typical 95% confidence limits of approximately ±15%.

Acknowledgements

We acknowledge financial support for this research from the Natural Sciences and Engineering Research Council of Canada (NSERC) in the form of research grants to CMC and scholarships to DPA, and support from the Canada Foundation for Innovation.

Appendix A. Supplementary data

Inversion transfer curves for the exchange of **8d** and $P(p\text{-}FC_6H_4)_3$ in various solvents and at different temperatures. Spin simulations for **8f** used to extract chemical shifts and coupling constants. Crystallographic data for the structural analysis have been deposited with the Cambridge Crystallographic Data Centre, CCDC No. 243198 for compounds **8c**, **8d**, **8e**, and **8f**. Copies of this information may be obtained free of charge from The Director, CCDC, 12

Union Road, Cambridge, CB2 1EZ UK, fax: int code +44 1223 336 033, or e-mail: deposit@ccdc.cam.ac.uk or www: http://www.ccdc.cam.ac.uk. Supplementary data associated with this article can be found, in the online version at doi:10.1016/j.jorganchem.2005.07.037.

References

[1] T.M. Trnka, R.H. Grubbs, Acc. Chem. Res. 34 (2001) 18.
[2] W.A. Herrmann, K. Ofele, D. Von Preysing, S.K. Schneider, J. Organomet. Chem. 687 (2003) 229.
[3] K.J. Cavell, D.S. McGuinness, Coord. Chem. Rev. 248 (2004) 671.
[4] C.M. Crudden, D.P. Allen, Coord. Chem. Rev. 248 (2004) 2247.
[5] M.S. Sanford, J.A. Love, R.H. Grubbs, J. Am. Chem. Soc. 123 (2001) 6543.
[6] P.E. Romero, W.E. Piers, R. McDonald, Angew. Chem., Int. Ed. 43 (2004) 6161.
[7] P.E. Romero, W.E. Piers, J. Am. Chem. Soc. 127 (2005) 5032.
[8] W.A. Herrmann, M. Elison, J. Fischer, C. Kocher, G.R.J. Artus, Angew. Chem., Int. Ed. 34 (1995) 2371.
[9] H. Lebel, M.K. Janes, A.B. Charette, S.P. Nolan, J. Am. Chem. Soc. 126 (2004) 5046.
[10] Part of the reason for the inactivity of **7** may be that the true catalyst is a mono-ligated Pd–NHC complex, but the high activity of the backbone metalated complex is intriguing.
[11] D.P. Allen, C.M. Crudden, L.A. Calhoun, R.Y. Wang, J. Organomet. Chem. 689 (2004) 3203.
[12] A.C. Chen, D.P. Allen, C.M. Crudden, R. Wang, A. Decken, Can. J. Chem. 83 (in press).
[13] With less bulky carbenes, a *trans* arrangement of phosphines is observed B. Cetinkaya, I. Ozdemir, P.H. Dixneuf, J. Organomet. Chem. 534 (1997) 153.
[14] G.A. Grasa, Z. Moore, K.L. Martin, E.D. Stevens, S.P. Nolan, V. Paquet, H. Lebel, J. Organomet. Chem. 658 (2002) 126.
[15] J. Halpern, Inorg. Chim. Acta. 50 (1981) 11.
[16] J. Halpern, T. Okamoto, A. Zakhariev, J. Mol. Catal. 2 (1976) 65.
[17] B.H. Lipshutz, B. Frieman, H. Birkedal, Org. Lett. 6 (2004) 2305.
[18] In preliminary experiments, we found the rate of exchange of **8a** to be similar to that of **8b**, but the limited solubility of **8a** under our conditions complicated the highly accurate determination of the rate of exchange.
[19] Phosphine dissociation studies were also performed in THF at 50 and 60 °C for **8d** and show the same rates of exchange observed in toluene.
[20] A.J. Arduengo, H.V.R. Dias, R.L. Harlow, M. Kline, J. Am. Chem. Soc. 114 (1992) 5530.
[21] C.A. Tolman, P.Z. Meakin, D.L. Lindner, J.P. Jesson, J. Am. Chem. Soc. (96) (1974) 2762.
[22] A.D. Bain, J.A. Cramer, J. Magn. Reson. 118A (1996) 21.